

Ecological speciation in sympatric palms: 4. Demographic analyses support speciation of *Howea* in the face of high gene flow

Alexander S. T. Papadopoulos,^{1,2}  Javier Igea,^{1,3}  Thomas P. Smith,¹ Ian Hutton,⁴ William J. Baker,⁵
Roger K. Butlin,^{6,7} and Vincent Savolainen^{1,5,8} 

¹Department of Life Sciences, Silwood Park Campus, Imperial College London, Ascot SL5 7PY, United Kingdom

²Molecular Ecology and Fisheries Genetics Laboratory, Environment Centre Wales, School of Natural Sciences, Bangor University, Bangor LL57 2UW, United Kingdom

³Department of Plant Sciences, University of Cambridge, Cambridge CB2 3EA, United Kingdom

⁴Lord Howe Island Museum, Lord Howe Island, New South Wales, Australia

⁵Royal Botanic Gardens, Kew, Richmond TW9 3AB, United Kingdom

⁶Department of Animal and Plant Sciences, University of Sheffield, Sheffield S10 2TN, United Kingdom

⁷Department of Marine Sciences, University of Gothenburg, Gothenburg SE-405 30, Sweden

⁸E-mail: v.savolainen@imperial.ac.uk

Received March 12, 2019

Accepted July 16, 2019

The idea that populations must be geographically isolated (allopatric) to evolve into separate species has persisted for a long time. It is now clear that new species can also diverge despite ongoing genetic exchange, but few accepted cases of speciation in sympatry have held up when scrutinized using modern approaches. Here, we examined evidence for speciation of the *Howea* palms of Lord Howe Island, Australia, in light of new genomic data. We used coalescence-based demographic models combined with double digest restriction site associated DNA sequencing of multiple individuals and provide support for previous claims by Savolainen et al. that speciation in *Howea* did occur in the face of gene flow.

KEY WORDS: Coalescence, ddRAD, speciation, sympatry.

Sympatric speciation has re-emerged as a controversial topic, with recent analyses of genome-wide data casting doubt on some of the best-known examples, such as cichlid fish in Cameroonian crater lakes (Martin et al. 2015). Due to a lack of confidence in ascertaining whether speciation has taken place in the face of gene flow, our understanding of the genomic underpinning of such processes has also remained piecemeal (Renaut et al. 2013; Cruickshank and Hahn 2014). Here, we examined a case of speciation in *Howea* palms, a genus that comprises only two species, both endemic to the subtropical Lord Howe Island (LHI; Savolainen et al. 2006). The island is isolated (600 km from mainland Australia) and minute (<16 km²). Furthermore, modeling of the geological history and sizes of LHI and nearby Ball's Pyramid rock showed that,

for any pair of endemic sister species that have diverged within the lifetime of the island, an allopatric phase in their divergence is unlikely (Papadopoulos et al. 2011). This was critical in promoting *Howea* as a prime example of sympatric speciation under a biogeographic definition, that is, speciation without geographic isolation (Savolainen et al. 2006; Mallet et al. 2009; Coyne 2011; Papadopoulos et al. 2011). Marked flowering time differences between the species indicate that prezygotic isolation is now strong and current levels of gene flow are likely to be low (Savolainen et al. 2006; Babik et al. 2009; Dunning et al. 2016; Hipperson et al. 2016). Indirect evidence of postzygotic isolation due to selection against juvenile hybrids supports the hypothesis that divergent selection has influenced the speciation process

(Hipperson et al. 2016). Given that the distributions of *Howea* palms overlap extensively and that they are wind pollinated, Savolainen et al. (2006) argued that speciation is likely to have occurred in the face of high gene flow, which may have reduced quickly as divergence progressed (Savolainen et al. 2006; Babik et al. 2009; Papadopulos et al., 2011, 2013b, 2014). However, previous efforts were based on a limited number of markers (two gene sequences and amplified fragment length polymorphism; Savolainen et al. 2006; Babik et al. 2009), which leaves room for doubt about the precise timing of divergence and did not allow for the quantification of the extent of the gene exchange between *Howea forsteriana* and *H. belmoreana*. Here, we characterize the demographic history of the *Howea* palms with a genome-wide dataset to evaluate (1) whether genomic data support speciation with gene flow and (2) how genetic exchange progressed during speciation in sympatry.

Materials and Methods

DNA EXTRACTION AND DOUBLE DIGEST RAD-SEQUENCING

Leaf tissue was collected and preserved in silica gel from 42 *H. belmoreana* and 54 *H. forsteriana* individuals sampled at Far Flats on LHI where both species co-occur. Genomic DNA was extracted from leaf tissue using DNeasy Plant Mini kits (Qiagen). Agarose gel electrophoresis was used to assess the quality of each DNA extract and DNA quantification was performed with a Qubit 2.0 fluorometer (Life Technologies). DNA samples were then processed following a modified version of the double digest RADseq protocol of Peterson et al. (2012). Digestion of the DNA template of each sample (250–1000 ng) was performed by combining the sample with 0.1 μL *EcoRI*-HF (10 U; NEB), 1 μL *MspI* (10U; NEB), 5 μL NEB buffer 4, and nuclease-free water to a total volume of 50 μL . Digestion reactions were incubated at 37°C for 3 hours. Digests were cleaned using the Agencourt AMPure XP bead clean up (Beckman Coulter) and quantified using a Qubit 2.0 fluorometer. Ligation of 6 base pairs (bp)-barcoded P1 (*EcoRI* overhang) and P2 (*MspI*) adaptors was performed in individual reactions composed of ca. 400 ng of the digested DNA product, 2 μL of each adaptor (4 nM), 2 μL T4 DNA ligase (4000 U; NEB), 4 μL 10 \times ligase buffer (NEB) and nuclease-free water to a total of volume 40 μL . Ligation reactions were incubated at 23°C for 30 min, followed by 65°C for 10 minutes, and then cooled to 18°C at a rate of 2°C/90 sec. Samples were pooled into batches of 12 containing compatible sets of barcodes, and cleaned using Agencourt AMPure XP beads. Each pool was size-selected between 344–408 bp using a Pippin Prep electrophoresis system (Sage Science). Each size-selected pool was PCR amplified in six to eight reactions each composed of 6 μL of DNA template, 2 μL of each ddRAD primer, 0.2 μL Phusion *Taq* polymerase (NEB),

0.4 μL dNTPs (10 mM; NEB), 4 μL 5 \times Phusion HF buffer (NEB), and 5.4 μL nuclease-free water. PCR reactions were run on a Veriti 96-Well Fast Thermal Cycler (Applied Biosystems) at 98°C for 30 sec, 12 cycles of 98°C for 15 sec, 65°C for 30 sec, 72°C for 30 sec, and final 72°C for 7 min. PCR reactions for each pool were combined and cleaned using Agencourt AMPure XP beads. Each cleaned pool was diluted to 4 nM and four pools with compatible barcodes were combined to produce libraries of 48 uniquely barcoded samples. Two ddRAD sequence libraries were prepared in this way. All libraries were sequenced to 100 bp, paired-end on an Illumina HiSeq 2500 (one lane per library) at the MRC Clinical Sciences Centre, Imperial College London. This generated an average of 6,186,469 reads per sample. Genotyping of ddRAD data was performed using the STACKS pipeline, building upon the catalogue generated in Papadopulos et al. (2019). To expand the catalogue to encompass haplotypes present in both *Howea* species, samples were assembled into loci using USTACKS (-m20, -M3) and these stacks were merged into the existing catalogue allowing three mismatches between loci in different individuals. To genotype individuals, loci were assembled with lower coverage in USTACKS (-m5, -M3) and these stacks were mapped to the catalogue loci.

DEMOGRAPHIC MODELLING

For the demographic analysis, the Far Flats individuals were genotyped at 4581 loci (23,109 single nucleotide polymorphisms; SNPs) with fewer than 20 missing individuals (minor allele frequency = 0.05). To account for missing data, we projected the number of individuals down to 36/54 *H. forsteriana* and 23/42 *H. belmoreana* and calculated the joint folded site frequency spectrum using $\delta a\delta i$ (Gutenkunst et al. 2009). We then inferred the demographic history of *Howea* from the site frequency spectrum using two methods: (1) the composite-likelihood framework implemented by *fastsimcoal2* (Excoffier et al. 2013) and (2) the diffusion approximation approach implemented in a modified version of $\delta a\delta i$ (Gutenkunst et al. 2009; Tine et al. 2014). This modified version of $\delta a\delta i$ accounts for variation in the rate of gene flow across the genome by dividing the genome into two types of loci (in P and 1-P proportions) with potentially different migration rates.

For *fastsimcoal2*, we estimated parameters 60 times for each of 10 demographic models to determine the combination of parameters with the highest likelihood. These models are shown in Figure 1A and assume either no population growth or population growth: model 1—speciation without gene flow; model 2—speciation with recent gene flow following secondary contact; model 3—speciation with initial gene flow; model 4—speciation with constant gene flow; and model 5—speciation with two distinct periods of migration where gene flow may vary. Model fit was assessed using the Akaike information criterion (AIC).

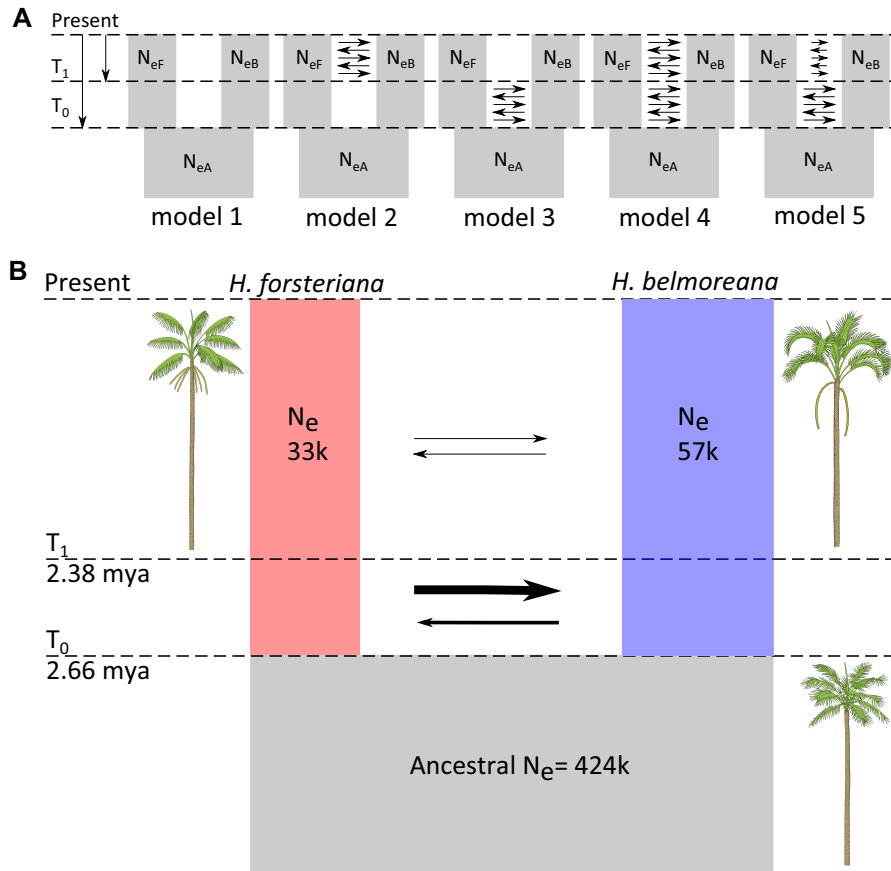


Figure 1. Coalescence analyses of demography in *Howea*. (A) Five models were tested, either assuming constant population sizes, allowing for exponential population growth through time, or heterogeneous migration across the genome (18 scenarios in total). Model 1: speciation without gene flow; 2: speciation with recent gene flow following secondary contact; 3: speciation with initial gene flow; 4: speciation with constant gene flow; and 5: species divergence with two periods where gene flow may vary. (B) Parameter estimates for the best fitting model with no growth estimated in *fastsimcoal2* (model 5).

Nonparametric bootstrapping (100 simulated datasets under the best model with 10 rounds of parameter estimation for each simulation) was used to estimate 95% confidence intervals for each parameter for the best model.

For $\delta a \delta i$, we compared the fit of the same 10 models as above plus another eight, that is, models 2–5 with and without population growth, but also including heterogeneous rates of migration across the genome. We ran two rounds of simulated annealing (one hot and one cold) followed by a final round of Broyden–Fletcher–Goldfarb–Shanno optimization. For each of the 18 models, we performed a minimum of 30 runs to ensure thorough estimation of the maximum likelihood and used AIC to perform model selection. For the best fitting model, we then ran 30 bootstrap replicates (ensuring that each replicate had at least 10 runs) using the built-in $\delta a \delta i$ procedure to get confidence intervals around the parameter estimates.

To calibrate the demographic models in *fastsimcoal2* and $\delta a \delta i$, we estimated the substitution rate in *Howea*. We first built a phylogenetic tree using genome wide data for all available palm

species. Transcriptome assemblies were obtained for *H. forsteriana* (Dunning et al 2016), *Elaeis guineensis*, and *E. oleifera* (African and American oil palms; Singh et al. 2013). Short read transcript data for *Phoenix dactylifera* (date palm; Al-Mssallem et al. 2013) were obtained from the short read archive (Accession Number SRR341952) and a transcriptome assembly was produced using *Trinity* (Grabherr et al. 2011) with default parameters and `min_kmer_cov` set to 2. *TransDecoder* was used to predict open reading frames (ORF) with a minimum length of 100 amino acids, and the longest ORF was selected. Reciprocal blast hits for all four palm species were established by collating reciprocal best blast results from a pair of species with the remaining two species; this rendered an initial set of orthologous alignments for the four species. An *M-coffee* (Wallace et al. 2006) pipeline was used to score these alignments. The nucleotide sequences were translated into protein using *t-coffee*, then the protein sequences were aligned with *MAFFT* (Katoh and Toh 2008), *Muscle* (Edgar 2004), *t-coffee* (Notredame et al. 2000), and *k-align* (Lassmann and Sonnhammer 2005) and translated back to DNA. Low-quality positions

with scores lower than 8 were trimmed. Protein alignments were used to guide gap placement in the nucleotide alignments. Finally, *maxalign* was used to check for any misaligned sequences in the alignments (Gouveia-Oliveira et al. 2007). Only alignments where all the orthologous sequences were properly aligned and deemed as high quality were retained and concatenated into a single file. *CODEML* (Yang 2007) was used to calculate fourfold degenerate sites, which are considered not to be subject to selection. Finally, *MCMCtree* (Yang 2007) was used to build a tree. To calibrate this tree, we used secondary calibrations from the most complete phylogenetic tree of the palm family (Baker and Couvreur 2013). Independent substitution rates were inferred for each branch in the tree, and HKY85 (the most complex substitution model available in *MCMCtree*) was selected. The MCMC chain was run to gather 20,000 samples after convergence had been achieved. The first 10,000 iterations were discarded as a burn-in. Assuming a generation time of 10 years for *Howea* palms (Lord Howe Island Nursery, pers. commun.), we estimated the rate of substitution of the branch leading to *H. forsteriana* to be 1.3×10^{-8} mutations per site per generation.

Results and Discussion

The demographic analyses provide strong support that *Howea* palms on LHI diverged in the face of ongoing gene flow. We have categorized the demographic models into four groups: (1) no population growth; (2) population growth; (3) no growth but heterogeneous migration across the genome; and (4) growth with heterogeneous migration across the genome. Using *fastsimcoal2*, where heterogeneous migration across the genome does not apply, model 5 (divergence with two periods where gene flow may vary) was most likely when no growth was modeled (Table 1). When population growth was permitted, model 5 was within 10 AIC from models 2 and 3, and therefore these three models are indistinguishable (Burnham and Anderson 2002) (Table 1). Using $\delta a\delta i$, model 5 was always the most likely model. However, when growth and heterogeneous migration across the genome were permitted, model 5 was indistinguishable from model 3 (speciation with initial gene flow; Table 1). The more complex growth models had smaller AIC than the no growth counterparts (Table 1), pointing to a period of exponential growth following species divergence. However, for both $\delta a\delta i$ and *fastsimcoal2*, the confidence intervals included the point estimates for all parameters only for the simplest scenario (i.e., without population size changes or heterogeneous rate of genome flow across the genome, Table S1). Other scenarios had greater levels of uncertainty indicating that our data were not sufficient to constrain such complex models and the point estimates for these models are likely to be unreliable. As the two demographic methods produced comparable results for the no growth scenarios, we focus our discussion on these simpler

cases. In models including two distinct periods of migration, we did not constrain the earlier migration rate to be higher than the more recent migration rate. Nevertheless, in all of these models the earlier rate of gene flow is estimated to be higher than more recent rates, supporting a reduction in gene flow during speciation. A similar pattern was found during the divergence of *Senecio* on Mt Etna (Filatov et al. 2016). In this study, the authors conducted a demographic analysis of two ragwort species (the low elevation *Senecio chrysanthemifolius* and high elevation *S. aethnensis*) along an altitudinal hybrid zone on Mt Etna. Their results were consistent with a scenario of speciation with gene flow and a divergence time that coincides with the rise of Mt. Etna to altitudes above 2000 m around 150,000 years ago (Filatov et al. 2016).

Figure 1B shows the detailed scenario for model 5 without growth. Confidence intervals for all parameters for $\delta a\delta i$ were much wider than for *fastsimcoal2* (Table S1), so we mainly discuss results from the latter. To assess the fit of the data to the model, we calculated the likelihood ratio G-statistic (composite likelihood ratio = 470.2) and compared this to the null distribution of simulated values (Excoffier et al. 2013). The observed value is in the tail of the simulated distribution (above the 99.9 percentile; range = 327.4–485.9). This is expected as these demographic models are a simplification of the real history of the species, whereas the null distribution is based on data simulated under the simple model (Excoffier et al. 2013).

Migration was initially two orders of magnitude higher from the smaller *H. forsteriana* population into the larger *H. belmoreana* lineage (proportion of migrants received per generation = 4.00×10^{-4} vs. 4.71×10^{-6} ; effective migrants per generation, $Nm = 13.01$ vs. 0.27). This initial period was followed by a reduction in gene flow (proportion of migrants received per generation = 1.6×10^{-7} vs. 3.3×10^{-7} ; $Nm = 0.01$ vs. 0.02). This is consistent with *H. forsteriana* being derived from a *belmoreana*-like ancestor that colonized a new habitat in which the *H. belmoreana* genetic background was selected against. The initially high Nm (mean = 6.64) is in the top 6% of values found in other examples of speciation with gene flow (range = 0.00–25.22, number of studies = 50, number of Nm values = 97; Pinho and Hey 2010; Filatov et al. 2016) and the proportion of migrants is similar to that found in the sympatric Nicaraguan cater lake cichlids (7.48×10^{-5} – 8.51×10^{-5} ; Kautt et al. 2016). These migration estimates fall below those expected under population genetic definitions of sympatric speciation ($m = 0.5$; Fitzpatrick et al. 2008). However, it is important to note that our migration estimates are averages over long periods of time, forced by a model that has an abrupt transition from one population to two populations. If we had a model that allowed a progressive reduction in gene flow, we may have seen values close to 0.5 at the start and then a rapid reduction as the initial barriers were built. Unfortunately, we do

Table 1. Summary statistics for model selection.

Model	Method	Max. Ln (likelihood)	No. of parameters	AIC	Delta AIC
1 (speciation without gene flow)	<i>fastsimcoal2</i>	-175,730	4	351,467	3092
2 (speciation with recent gene flow following secondary contact)	<i>fastsimcoal2</i>	-174,992	7	349,997	1622
3 (speciation with initial gene flow)	<i>fastsimcoal2</i>	-175,522	7	350,109	1734
4 (speciation with constant gene flow)	<i>fastsimcoal2</i>	-175,049	6	351,059	2683
5 (species divergence with two periods where gene flow may vary)	<i>fastsimcoal2</i>	-174,955	9	349,928	1552
1 + growth	<i>fastsimcoal2</i>	-174,898	6	349,808	1433
2 + growth	<i>fastsimcoal2</i>	-174,179	9	348,375	0
3 + growth	<i>fastsimcoal2</i>	-174,181	9	348,377	2
4 + growth	<i>fastsimcoal2</i>	-174,265	8	348,548	173
5 + growth	<i>fastsimcoal2</i>	-174,180	11	348,382	7
1	$\Delta a\delta i$	-2602.12	4	5210	2705
2	$\delta a\delta i$	-2051.04	7	4114	1609
3	$\delta a\delta i$	-2055.46	7	4123	1617
4	$\delta a\delta i$	-2067.86	6	4146	1640
5	$\delta a\delta i$	-2012.61	9	4041	1536
1 + growth	$\delta a\delta i$	-1747.95	6	3506	1000
2 + growth	$\delta a\delta i$	-1384.78	9	2786	280
3 + growth	$\delta a\delta i$	-1427.55	9	2871	366
4 + growth	$\delta a\delta i$	-1431.38	8	2877	371
5 + growth	$\delta a\delta i$	-1377.74	11	2775	270
2 + heterogeneous M	$\delta a\delta i$	-1741.57	10	3501	996
3 + heterogeneous M	$\delta a\delta i$	-1786.64	10	3591	1086
4 + heterogeneous M	$\delta a\delta i$	-1785.31	9	3587	1081
5 + heterogeneous M	$\delta a\delta i$	-1730.07	14	3486	981
2 + growth + heterogeneous M	$\delta a\delta i$	-1255.63	12	2533	28
3 + growth + heterogeneous M	$\delta a\delta i$	-1241.78	12	2506	0
4 + growth + heterogeneous M	$\delta a\delta i$	-1256.03	11	2532	26
5 + growth + heterogeneous M	$\delta a\delta i$	-1239.00	16	2508	2

The best fitting models within each class (with or without growth and heterogeneous migration) are highlighted in bold. In classes where the Delta AIC for multiple was <10, the best set of models is in bold.

not have the data to fit such a model. Of course, it would also have strong heterogeneity across the genome.

Based on a generation time of 10 years, we found that the species initially diverged roughly 2.7 million years ago, which is older than previously estimated by phylogenetic analysis of two genes (1.92 ± 0.52 million years ago; Savolainen et al. 2006). Allowing for different rates of migration across the genome (using $\delta a\delta i$) resulted in a more recent divergence time than other models at 1.41 million years ago, but this fell outside the bootstrap confidence intervals. Our estimates predate the proposed mid-Pleistocene age of the current calcareous deposits of the island (Brooke 2003; Woodroffe et al. 2006; Papadopulos et al. 2013a). It is possible that colonization was on calcareous soils predating those currently on the island, and which would have eroded since then. Alternatively, colonization of mid-Pleistocene

calcareous sites may have taken place after divergence with the initial selection pressures stemming from other sources, such as water availability or salinity (Papadopulos et al. 2013b). The timing of the shift to a lower migration rate differs substantially between the methods; *fastsimcoal2* points to a large reduction in migration $\sim 40,000$ years after initial divergence, whereas $\delta a\delta i$ indicates smaller change that took place much more recently (100,000 year after divergence). Estimates of current population sizes (*H. forsteriana* $N_e = 32,510$; *H. belmoreana* $N_e = 57,181$) are similar to the estimated census population size (all LHI *Howea* $\sim 100,000$, with 2.7 times as many *H. belmoreana* as *H. forsteriana*) (Savolainen et al. 2006; Hipperson et al. 2016). The *fastsimcoal2* estimated ancestral N_e (424,288) is within the bounds of possibility, but is likely to be an overestimate as variation in coalescence time due to selection in the ancestral species may cause *fastsimcoal2*

to explain excess variance by inferring very large N_e . The $\delta a \delta i$ ancestral N_e was an order of magnitude lower (12,570), and it is therefore unclear which estimate is best. It seems likely that small initial colonizing group came from a large mainland population and then grew rapidly, but it is not possible to determine with our analyses.

The inconsistent results for the more complex models show that our analyses are limited by the data. Refinements could be made using whole genome re-sequencing data, although the large genome size and complexity makes this challenging. Additionally, more detailed data would allow the inclusion of other parameters in more complex frameworks that have emerged recently such as that of Roux et al (2016), which models heterogeneity in coalescence times due to selection.

Currently, reproductive isolation between the species is strong, although not complete given that occasional fertile hybrids are formed (Babik et al. 2009). Our results are consistent with the idea that initial local adaptation and postzygotic isolation were supplemented by the rapid completion of prezygotic isolation through flowering time differences (Papadopoulos et al. 2013b, 2014). Furthermore, given the supporting evidence these results allow us to rule out continuous absence of gene flow, even though LHI was larger at the time of speciation (Papadopoulos et al., 2011, 2013a; Linklater et al. 2018). Unlike recent genomic reanalyses of classic cases of speciation in sympatry, our results support the proposition that *Howea* palms must have diverged with continuous gene flow. We note, however, that genomic data by themselves may only permit the rejection of the simplest form of allopatry (Yang et al. 2017). In this sense, our demographic analyses should be seen in concert with other lines of evidence such as the geological history of LHI, lack of population structure on LHI, and the finding of candidate reproductive isolation genes (Dunning et al. 2016). Furthermore, our analyses indicate that divergence may have predated the origin of the calcarenite soils on LHI, and therefore identifying candidate “speciation genes” with functions related to drought and salt tolerance may be more important than extremes of pH.

AUTHOR CONTRIBUTIONS

VS designed the research with contributions from ASTP, JI, and RKB. ASTP and TPS collected data. ASTP and JI analyzed the data. IH and WB contributed to field collections. ASTP and VS wrote the manuscript. All authors commented on the manuscript.

ACKNOWLEDGMENTS

We thank the Lord Howe Island Board and the New South Wales National Park and Wildlife Services for granting research permits, Hank and Sue Bower, Christo Haselden, Peter Weston, Larry Wilson for their help on LHI, Laszlo Csiba and Helen Hipperson for help in the lab, Matt Hahn for comments, and the European Research Council, NERC and the Leverhulme Trust for funding.

DATA ARCHIVING

The sequence data are available at the Sequence Reads Archive under accession numbers PRJNA386480 and SRP063985. Data available from the Dryad Digital Repository: <https://doi.org/10.5061/dryad.s3t2qn0>.

REFERENCES

- Al-Mssallem, I. S., S. Hu, X. Zhang, Q. Lin, W. Liu, J. Tan, X. Yu, J. Liu, L. Pan, T. Zhang, et al. 2013. Genome sequence of the date palm phoenix dactylifera L. *Nat. Commun.* 4:2274.
- Babik, W., R. K. Butlin, W. J. Baker, A. S. T. Papadopoulos, M. Boulesteix, M. C. Anstett, C. Lexer, I. Hutton, and V. Savolainen. 2009. How sympatric is speciation in the *Howea* palms of Lord Howe Island? *Mol. Ecol.* 18:3629–3638.
- Baker, W. J., and T. L. P. Couvreur. 2013. Global biogeography and diversification of palms sheds light on the evolution of tropical lineages. I. Historical biogeography. *J. Biogeogr.* 40:274–285.
- Brooke, B. 2003. Quaternary calcarenite stratigraphy on Lord Howe Island, southwestern Pacific Ocean and the record of coastal carbonate deposition. *Quat. Sci. Rev.* 22:859–880.
- Burnham, K. P., and D. R. Anderson. 2002. Model selection and multimodel inference: a practical information-theoretic approach. Springer, New York.
- Coyne, J. A. 2011. Speciation in a small space. *Proc. Natl. Acad. Sci. USA* 108:12975–12976.
- Cruickshank, T. E., and M. W. Hahn. 2014. Reanalysis suggests that genomic islands of speciation are due to reduced diversity, not reduced gene flow. *Mol. Ecol.* 23:3133–3157.
- Dunning, L. T., H. Hipperson, W. J. Baker, R. K. Butlin, C. Devaux, I. Hutton, J. Igea, A. S. T. Papadopoulos, X. Quan, C. M. Smadja, et al. 2016. Ecological speciation in sympatric palms: 1. Gene expression, selection and pleiotropy. *J. Evol. Biol.* 29:1472–1487.
- Edgar, R. C. 2004. MUSCLE: multiple sequence alignment with high accuracy and high throughput. *Nucleic Acids Res.* 32:1792–1797.
- Excoffier, L., I. Dupanloup, E. Huerta-Sánchez, V. C. Sousa, and M. Foll. 2013. Robust demographic inference from genomic and SNP data. *PLoS Genet.* 9:e1003905.
- Filatov, D. A., O. G. Osborne, and A. S. T. Papadopoulos. 2016. Demographic history of speciation in a *Senecio* altitudinal hybrid zone on Mt. Etna. *Mol. Ecol.* 25:2467–2481.
- Fitzpatrick, B. M., J. A. Fordyce, and S. Gavrillets. 2008. What, if anything, is sympatric speciation? *J. Evol. Biol.* 21:1452–1459.
- Gouveia-Oliveira, R., P. W. Sackett, and A. G. Pedersen. 2007. MaxAlign: maximizing usable data in an alignment. *BMC Bioinformatics* 8:312.
- Grabherr, M. G., B. J. Haas, M. Yassour, J. Z. Levin, D. A. Thompson, I. Amit, X. Adiconis, L. Fan, R. Raychowdhury, and Q. Zeng. 2011. Full-length transcriptome assembly from RNA-Seq data without a reference genome. *Nat. Biotechnol.* 29:644–652.
- Gutenkunst, R. N., R. D. Hernandez, S. H. Williamson, and C. D. Bustamante. 2009. Inferring the joint demographic history of multiple populations from multidimensional SNP frequency data. *PLoS Genet.* 5: e1000695.
- Hipperson, H., L. T. Dunning, W. J. Baker, R. K. Butlin, I. Hutton, A. S. T. Papadopoulos, C. M. Smadja, T. C. Wilson, C. Devaux, and V. Savolainen. 2016. Ecological speciation in sympatric palms: 2. Pre- and post-zygotic isolation. *J. Evol. Biol.* 29:2143–2156.
- Katoh, K., and H. Toh. 2008. Recent developments in the MAFFT multiple sequence alignment program. *Brief. Bioinform.* 9:286–298.
- Kautt, A. F., G. Machado-Schiaffino, and A. Meyer. 2016. Multispecies outcomes of sympatric speciation after admixture with the source population in two radiations of nicaraguan crater lake cichlids. *PLoS Genet.* 12:1–33.

- Lassmann, T., and E. L. L. Sonnhammer. 2005. Kalign—an accurate and fast multiple sequence alignment algorithm. *BMC Bioinformatics* 6:298.
- Linklater, M., S. M. Hamylton, B. P. Brooke, S. L. Nichol, A. R. Jordan, and C. D. Woodroffe. 2018. Development of a seamless, high-resolution bathymetric model to compare reef morphology around the subtropical island shelves of lord howe island and balls pyramid, Southwest Pacific Ocean. *Geosciences* 8:11.
- Mallet, J., A. Meyer, P. Nosil, and J. L. Feder. 2009. Space, sympatry and speciation. *J. Evol. Biol.* 22:2332–2341.
- Martin, C. H., J. S. Cutler, J. P. Friel, C. D. Touokong, G. Coop, and P. C. Wainwright. 2015. Complex histories of repeated gene flow in Cameroon crater lake cichlids cast doubt on one of the clearest examples of sympatric speciation. *Evolution* 69:1406–1422.
- Notredame, C., D. G. Higgins, and J. Heringa. 2000. T-Coffee: a novel method for fast and accurate multiple sequence alignment. *J. Mol. Biol.* 302:205–217.
- Papadopoulos, A. S. T., W. J. Baker, D. Crayn, R. K. Butlin, R. G. Kynast, I. Hutton, and V. Savolainen. 2011. Speciation with gene flow on Lord Howe Island. *Proc. Natl. Acad. Sci. USA* 108:13188–13193.
- Papadopoulos, A. S. T., W. J. Baker, and V. Savolainen. 2013a. Sympatric speciation of island plants: the natural laboratory of Lord Howe Island. Pp. 37–57 in P. Michalak, ed. *Speciation: natural processes, genetics & biodiversity*. Nova Science, New York, NY.
- Papadopoulos, A. S. T., Z. Price, C. Devaux, H. Hipperson, C. M. Smadja, I. Hutton, W. J. Baker, R. K. Butlin, and V. Savolainen. 2013b. A comparative analysis of the mechanisms underlying speciation on Lord Howe Island. *J. Evol. Biol.* 26:733–745.
- Papadopoulos, A. S. T., M. Kaye, C. Devaux, H. Hipperson, J. Lighten, L. T. Dunning, I. Hutton, W. J. Baker, R. K. Butlin, and V. Savolainen. 2014. Evaluation of genetic isolation within an island flora reveals unusually widespread local adaptation and supports sympatric speciation. *Philos. Trans. R. Soc. B Biol. Sci.* 369:20130342.
- Papadopoulos, A. S. T., J. Igea, L. T. Dunning, O. G. Osborne, X. Quan, J. Pellicer, C. Turnbull, I. Hutton, W. J. Baker, R. K. Butlin, et al. 2019. Ecological speciation in sympatric palms: 3. Genetic map reveals genomic islands underlying species divergence in *Howea*. *Evolution*. Online Early:XX–XX.
- Peterson, B. K., J. N. Weber, E. H. Kay, H. S. Fisher, and H. E. Hoekstra. 2012. Double digest RADseq: an inexpensive method for de novo SNP discovery and genotyping in model and non-model species. *PLoS One* 7:e37135.
- Pinho, C., and J. Hey. 2010. Divergence with gene flow: Models and data. *Annu. Rev. Ecol. Evol. Syst.* 41:215–230.
- Renaut, S., C. J. Grassa, S. Yeaman, B. T. Moyers, Z. Lai, N. C. Kane, J. E. Bowers, J. M. Burke, and L. H. Rieseberg. 2013. Genomic islands of divergence are not affected by geography of speciation in sunflowers. *Nat. Commun.* 4:1827.
- Roux, C., C. Fraïsse, J. Romiguier, Y. Anciaux, N. Galtier, and N. Bierne. 2016. Shedding light on the grey zone of speciation along a continuum of genomic divergence. *PLoS Biol.* 14:1–22.
- Savolainen, V., M.-C. Anstett, C. Lexer, I. Hutton, J. J. Clarkson, M. V. Norup, M. P. Powell, D. Springate, N. Salamin, and W. J. Baker. 2006. Sympatric speciation in palms on an oceanic island. *Nature* 441:210–213.
- Singh, R., M. Ong-Abdullah, E.-T. L. Low, M. A. A. Manaf, R. Rosli, R. Nookiah, L. C.-L. Ooi, S.-E. Ooi, K.-L. Chan, M. A. Halim, et al. 2013. Oil palm genome sequence reveals divergence of interfertile species in old and new worlds. *Nature* 500:335–339.
- Tine, M., H. Kuhl, P. A. Gagnaire, B. Louro, E. Desmarais, R. S. T. Martins, J. Hecht, F. Knaust, K. Belkhir, S. Klages, et al. 2014. European sea bass genome and its variation provide insights into adaptation to euryhalinity and speciation. *Nat. Commun.* 5:5770.
- Wallace, I. M., O. O’Sullivan, D. G. Higgins, and C. Notredame. 2006. M-Coffee: combining multiple sequence alignment methods with T-Coffee. *Nucleic Acids Res.* 34:1692–1699.
- Woodroffe, C. D., D. M. Kennedy, B. P. Brooke, and M. E. Dickson. 2006. Geomorphological evolution of Lord Howe Island and carbonate production at the latitudinal limit to reef growth. *J. Coast. Res.* 22:188–201.
- Yang, M., Z. He, and S. Shi. 2017. Can genomic data alone tell us whether speciation happened with gene flow? *Mol. Ecol.* 26:2845–2849.
- Yang, Z. 2007. PAML 4: phylogenetic analysis by maximum likelihood. *Mol. Biol. Evol.* 24:1586–1591.

Associate Editor: B. Emerson
Handling Editor: D. Hall

Supporting Information

Additional supporting information may be found online in the Supporting Information section at the end of the article.

Table S1. Inferred parameters for the selected model 5.